

LIDAR SOUNDINGS OF NOCTILUCENT CLOUDS AND TEMPERATURES DURING DAY AND NIGHT IN THE SUMMER MID-LATITUDE MIDDLE ATMOSPHERE

Maren Kopp, Michael Gerding, Josef Höffner, Marius Zecha, and Franz-Josef Lübken

Leibniz-Institute of Atmospheric Physics, Schlossstr. 6, 18225 Kühlungsborn, Germany

ABSTRACT

At the Leibniz-Institute of Atmospheric Physics in Kühlungsborn (54°N, 12°E) we have developed a day-time capable Rayleigh-Mie-Raman (RMR) lidar for the mesosphere. Temperature soundings are feasible up to approximately 75 km during the day and up to 90 km during the night. Furthermore, measurements are performed at high solar elevation angles of up to $\sim 60^\circ$. In 2010 we performed first daylight observations, covering the whole June-July summer season. In this paper we present first results on absolute temperatures and their variation by e.g. gravity waves and tides. Daylight RMR soundings allow simultaneous observations of ice particles together with the OSWIN-VHF radar. OSWIN observes so-called Mesospheric Summer Echoes which require a sufficient electron density beside the existence of ice particles.

Key words: Rayleigh-Mie-Raman-Lidar; Noctilucent Clouds, Mesospheric Summer Echoes.

1. INTRODUCTION

Lidar soundings of the middle atmosphere are often limited to nighttime conditions. During the day, the solar background radiation results in a much too high noise level. Summer soundings at mid-latitudes during night are limited to 4-5 h. By this, lidars provide only an incomplete picture of the atmosphere. Tides systematically change temperatures. Thus, a full diurnal coverage is required to analyse tidal parameters. Gravity waves and tides play an important role to understand the processes in the atmosphere due to the fact that they influence the dynamic and temperature structure [1].

Continuous nighttime temperature measurements are performed with a combined Rayleigh-Mie-Raman (RMR) lidar and a Potassium Resonance lidar since 2002 in Kühlungsborn [2]. An altitude range from 0 km to ~ 105 km is covered. Consequently, these continuous, combined lidar measurements allowed an analysis of wave structures from the troposphere up to the lower thermosphere at the IAP [3, 4]. A first climatology from these temperature measurements was published in 2007 [5].

Lidar measurements during daylight are only done by a

few lidar stations e. g. [6, 7, 8, 9]. The technique of day-time capability is quite rare, especially for observations up to the mesosphere and at high solar elevation angles. Daytime capability at Kühlungsborn has been realized already for the Potassium Resonance lidar with a so-called Faraday-Anomalous-Dispersion-Optical-Filter (FADOF) since several years [10]. Observations are made from an altitude of 80 to ~ 105 km. For combined soundings of a greater altitude range, at first from 40 to ~ 105 km, a new RMR lidar was developed. First daylight NLC soundings were performed with the new RMR lidar in 2009 whereas the first daylight temperature soundings started in 2010. In order to achieve daylight capability, enormous technical efforts are necessary to reduce the background and to keep the signal as high as possible. In section 2 and 3 we present how we realized the background suppression and show an example of the observed background under daylight conditions. Daylight lidar measurements allow simultaneous observations of Noctilucent Clouds (NLC) by RMR-lidar and Mesospheric Summer Echoes (MSE) by the OSWIN-VHF-radar [11, 12]. An example of a combined NLC and MSE observation is shown in section 4. Temperatures during night and day are presented in section 5. Concluding in section 6 we present first results of a tidal analysis, shown as a case study for June 2010.

2. DAYLIGHT LIDAR MEASUREMENTS

For lidar observations during daylight a new RMR lidar has been developed and installed at our site, operating independently from the old (nighttime-only) RMR lidar. We use a Nd:YAG laser (Newport PRO series) with a beam divergence of less than 0.5 mrad. The divergence is further reduced to about 60 μ rad with a beam widening telescope.

The lidar beam is coaxially (with the telescope) transmitted into the atmosphere so that we achieve a full overlap over the whole altitude range. Atmospheric turbulence and jitter require a fast beam-stabilization to fix the laser beam within a small Field of View (FOV), that is about 60 μ rad comparable to the laser divergence. Comparable conventional lidars have greater FOV's, about 1000 μ rad. A small FOV is preferable for daylight measurements because this results in a lower background. The technique

of a fast pulse to pulse beam-stabilization is adopted from a solution for our mobile iron lidar [13]. The remaining jitter is about $5 \mu\text{rad}$.

Spectral filtering is used in order to reduce the background further by applying a narrowband interference filter (IF), and two Fabry-Perot-Etalons (FPE). The IF has a Full Width Half Maximum (FWHM) of 130 pm and blocks the light by 5 orders of magnitude. Both etalons have similar optical properties. The first etalon has a Free Spectral Range (FSR) of 120 pm and a FWHM of ~ 4 pm. The FSR for the second etalon is 140 pm and the FWHM is about 4.5 pm. The effective etalon finesse (FSR / FWHM) is about 30. Spectral filters like FPEs influences the temperature calculations and thus a transmission correction is needed. The etalon transmission function (so-called Airy-function) has to be known exactly for an adequate correction. We achieved a very high transmission of greater than 90% for both etalons. The transmission curves of the two etalons fit well to an Airy function, the basis of a good transmission correction mentioned before [14].

3. BACKGROUND VARIATION DURING DAY AND NIGHT

Figure 1 shows the background variation for our daytime and nighttime RMR-detectors. The peaks between 10 UT and 15 UT are due to clouds drifting through the lidar FOV. The RMR nighttime detector is switched on at ~ 20.45 UT, after the background is low enough to make measurements. Before that time the background goes beyond 200 cts / 4000 pulses (in a 200 m bin), and allows no measurement (shown as the dashed black line). Near civil twilight (-6°) the background drops by several orders of magnitude. A measurement with the nighttime detector is possible until ~ 2.15 UT. The increasing background stops the measurement. This is shown as a simulated background (black dashed line) in the plot, because no observation takes place at this time. In contrast the background from the RMR daytime detector is low while the elevation is lower than 0° , much less influenced by twilight. The maximum background is about 220 cts / 4000 pulses at 12 UT.

4. SIMULTANEOUS OBSERVATION OF NLC AND MSE

Mesospheric Summer Echoes (MSE) originate from backscatter of radar waves from free electrons influenced by charged ice particles in the mesopause region. MSE are mostly observed during daytime due to the required electron densities. Despite all progress being made in the last few years there are still several open questions regarding the relation of NLC and MSE at mid-latitudes. The equivalent phenomena at polar latitudes PMSE are much more frequent and thus better observed and analyzed [15, 16].

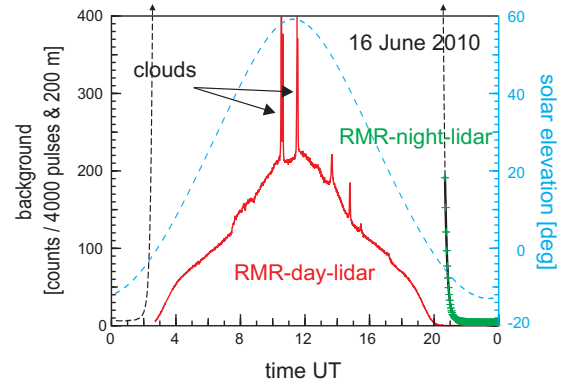


Figure 1. Background variation for the daytime Rayleigh-Mie-Raman (RMR) detector (red) and the nighttime RMR detector (green), 16 June 2010. The dashed black lines show a simulated background for the nighttime detector. At these times no observations are possible because the background increases by many orders of magnitude. The dashed blue line shows the solar elevation.

In combined lidar / radar observations at IAP were shown that ice particles e. g. mostly occur during southward winds [17]. Simultaneous observations of MSE and NLC require daytime lidar capabilities that are possible with the RMR lidar only since 2009. Figure 2 shows a combined observation of a NLC observed by lidar, and a MSE observed by radar. In this example MSE occur in a greater altitude range (between 80 km and 85 km) whereas the NLC covers the lower part (between 79 and 83 km). The lower edges of the NLC and the MSE agree well. Exceptions are due to the different FOVs of the lidar and radar system. Lower edges of NLC and MSE are often sharp as expected from observations from polar latitudes, whereas the upper edge is blurred because ice particles need a certain size in order to be detected by a lidar [18, 19]. In nine years of combined observations at ALOMAR in Northern Norway (69°N , 16°E) were shown that e. g. the PMSE occurrence rate of $\sim 75\%$ is clearly higher than the NLC occurrence rate with $\sim 20\%$ [20].

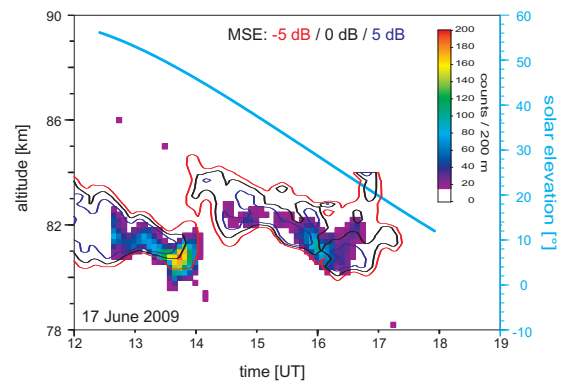


Figure 2. Simultaneous observation (17 June 2009) of a Noctilucent Cloud, shown as filled color contour structure and a Mesospheric Summer Echo, shown as open contour lines. The blue line indicates the solar elevation.

5. TEMPERATURE VARIATION DURING DAY AND NIGHT

Figure 3 shows temperatures during night and day in the upper stratosphere and mesosphere, taken from the daytime capable RMR lidar. The start value for the temperature retrieval at the upper edge of the Rayleigh integration range is delivered by the Potassium Resonance lidar (potassium temperatures are not plotted). As can be seen from Fig. 3 we are capable of measuring temperature profiles from 40 km up to 75 km during the day with an integration time of 1 h and a smoothing of 2 km. In future we will apply an additional detector to calculate temperatures below 40 km in the lower stratosphere. At night temperatures are observed up to an altitude of 90 km. Temperatures in the mesopause region, above 80 km, are as low as 160 K. Temperature variations are due to tides and gravity waves. In the following we present first results of a tidal analysis.

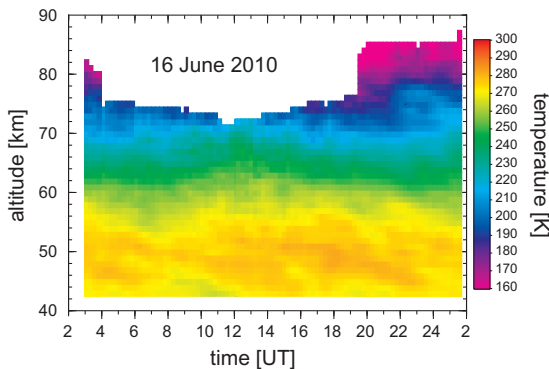


Figure 3. Temperatures during day and night as observed by the daylight Rayleigh-Mie-Raman lidar (16 June 2010)

6. FIRST RESULTS IN TIDAL ANALYSIS

Full diurnal coverage allows for the first time a tidal analysis from our temperature data. The analysis is done with a composite of 11 days in June 2010. We calculate tidal components between an altitude range of 40 to 70 km. The available data is averaged for each particular time and altitude. Figure 4 shows all individual temperatures from 11 days at an altitude of 50 km. The individual data show the natural variability caused by e. g. gravity and planetary waves. The red line is a combined fit of a semidiurnal and a diurnal variation. For this June example the measured diurnal amplitude is ~ 3 K, approximately 3 times larger than the semidiurnal amplitude (~ 1 K) for an altitude of 50 km. This plot shows a nice agreement of the data points and the harmonic fit. An analysis is possible for every altitude within the range from 40 to 70 km.

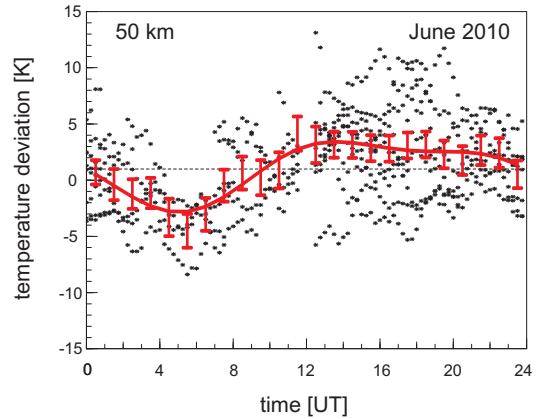


Figure 4. Temperature deviations for an altitude of 50 km in June 2010 from a composite of 11 days. The black points show the individual temperature data. The red bars characterize the measured values in addition to the variability of the measurement. The red line is a combined fit of a semidiurnal and a diurnal variation.

7. CONCLUSIONS

In this paper we have shown first results of the new daylight capable RMR-lidar in Kühlungsborn. This new lidar enables temperature and NLC measurements at solar elevations up to 60° , i.e. during high background from the Sun. In order to reduce the solar background we applied a small FOV of $60 \mu\text{rad}$. Furthermore, we used two narrowband Fabry-Perot Etalons in a high transmission configuration of greater than 90%. During daylight we are able to perform temperature measurements up to 75 km, and up to 90 km at night. We presented a first case of a simultaneous measured NLC and MSE in 2009. This comparison is only possible with our daylight capable lidar system because MSE only occur at daytime. At night the electron density is too low to produce significant radar backscatter. Furthermore we have shown first results of a harmonic tidal analysis in temperature data for 11 days in June 2010. The harmonic fit of the semidiurnal and diurnal tidal component agrees well with the observed variation. In future we would like to complete a seasonal cycle of tidal parameters with a larger database.

8. ACKNOWLEDGMENTS

We thank T. Köpnick and M. Priester for their help with the development and operation of the lidar systems.

REFERENCES

- [1] Fritts D. C., Alexander M. J. (2003). Gravity wave dynamics and effects in the middle atmosphere. *Rev. Geophys.*, 41(1), 1013, doi: 10.129/2001RG000106.
- [2] Alpers M., Eixmann R., Fricke-Begemann C., et al. (2004). Temperature lidar measurements from 1 to 105 km altitude using resonance, Rayleigh, and Rotational Raman Scattering. *Atmos. Chem. Phys.*, 4, 793–800.
- [3] Rauthe M., Gerding M., Höffner J., et al. (2006). Lidar temperature measurements of gravity waves over Kühlungsborn (54°N) from 1 to 105 km: A winter-summer comparison. *J. Geophys. Res.*, 111, D24108.
- [4] Rauthe M., Gerding M., and Lübken F.-J. (2008). Seasonal changes in gravity wave activity measured by lidars in midlatitudes. *Atmos. Chem. Phys.*, 8, 6775–6787.
- [5] Gerding M., Höffner J., Lautenbach J., et al. (2008). Seasonal variation of nocturnal temperatures between 1 and 105 km altitude at 54°N observed by lidar. *Atmos. Chem. Phys.*, 8, 7465–7482.
- [6] Fiedler J., von Cossart G., and von Zahn U. (1999). Stratospheric/mesospheric temperature profiles obtained by the ALOMAR RMR lidar over Andoya. *European Rocket and Balloon Programs and Related Research, Proceedings of the 14th ESA Symposium, Potsdam, Germany*. 437, p.263, ESASP.437.263F.
- [7] Chu X., Pan W., Papen G. C., et al. (2002). Fe Boltzmann temperature lidar: design, error analysis, and initial results at the North and South Poles. *Appl. Opt.*, 41, 4400–4410.
- [8] Klekociuk A. R., Lambert M. M., Vincent R. A., et al. (2003). First year of Rayleigh lidar measurements of middle atmosphere temperatures above Davis, Antarctica. *Adv. Space Res.*, 32(5), 771–776.
- [9] Thayer J. P., Rapp M., Gerrard A. G., et al. (2003). Gravity-wave influences on Arctic mesospheric clouds as determined by a Rayleigh lidar at Sondrestrom, Greenland. *J. Geophys. Res.*, 108(D8).
- [10] Höffner J. and Fricke-Begemann C. (2005). Accurate lidar temperatures with narrowband filters. *Opt. Lett.*, 30, 890–892.
- [11] Latteck R., Singer W., and Höffner J. (1999). Mesosphere summer echoes as observed by VHF radar at Kühlungsborn (54°N). *Geophys. Res. Lett.*, 26(11), 1533–1536.
- [12] Zecha M., Bremer J., Latteck R., et al. (2003). Properties of midlatitude mesosphere summer echoes after three seasons of VHF radar observations at (54°N). *J. Geophys. Res.*, 108(D8), 8439.
- [13] Höffner J. and Lautenbach J. (2009). Daylight measurements of mesopause temperature and vertical wind with the mobile scanning iron Lidar. *Opt. Lett.*, 34(9), 1351–1353.
- [14] Gerding M., Höffner J., Kopp M., et al. (2010). Mesospheric temperature and aerosol soundings during day and night: Spectral and spatial filtering techniques. *In Reviewed and revised papers at the 25th International Laser Radar Conference, St. Petersburg, Russia*, 67–70.
- [15] Rapp M. and Lübken F.-J. (2004). Polar mesosphere summer echoes (PMSE): review of observations and current understanding. *Atmos. Chem. Phys.*, 4, 2601–2633.
- [16] Cho J. Y. N., and Röttger J. (1997). An updated review of polar mesosphere summer echoes: Observation, theory, and their relationship to noctilucent clouds and subvisible aerosols. *J. Geophys. Res.*, 102(D2), 2001–2020.
- [17] Gerding M., Höffner J., Rauthe M., et al. (2007). Simultaneous observation of noctilucent clouds, mesospheric summer echoes, and temperature at a midlatitude station (54° N). *J. Geophys. Res.*, 112(D12111).
- [18] Lübken F.-J., Zecha M., and Höffner J. (2004). Temperatures, polar mesosphere summer echoes, and noctilucent clouds over Spitsbergen (78° N). *J. Geophys. Res.*, 109(D11203).
- [19] Lübken F.-J., Lautenbach J., Höffner J., et al. (2009). First continuous temperature measurements within polar mesosphere summer echoes. *J. Atmos. Solar-Terr. Phys.*, 71, 453–463.
- [20] Kaifler N., Baumgarten G., Fiedler J., et al. (2011). Coincident measurements of PMSE and NLC above ALOMAR (69° N, 16°E) by Radar and Lidar from 1999–2008. *Atmos. Chem. Phys.*, 11, 1355–1366.